# AGC regulation capability prediction and optimization of coal-fired thermal power plants

Fei Jin, Xiaoguang Hao, Wenbin Zhang, Mingkai Weng and Bin Wu*

State Grid Hebei Energy Technology Service Co Ltd., Shijiazhuang, China

The improvement of the AGC regulation capability of thermal power plants is very important for the secure and stable operation of the power grid, especially in the situation of large-scale renewable energy access to the power grid. In this study, the prediction and optimization for the AGC regulation capability of thermal power plants is proposed. Firstly, considering parameters related to the AGC regulation of the thermal power plant, the max-relevance and min-redundancy (mRMR) is used to extract features from historical sequences of the parameters. Next, a model with multi-long short-term neural networks (mLSTM) is constructed to predict the AGC regulation capability; that is, the obtained feature set is considered as the inputs of the first LSTM sub-model to predict future values of the main steam pressure and main steam temperature, which are then utilized as the inputs of the second LSTM sub-model to predict the actual power generation during AGC regulation operation. Then, the AGC regulation index is calculated according to the "management rules of grid-connected operation of power plant in Northern China" and "management rules of auxiliary service of the grid-connected power plant in Northern China" (i.e., "two rules"), and it is then considered as the objective function to be maximized by optimizing the coal feed rate, air supply rate, and feedwater flow rate. Finally, the actual AGC regulation process of a 300 MW coal-fired power plant is used as an application, and the results show that the proposed method can effectively predict and improve the regulation capability when the AGC instruction is received from the power grid.

# 1 Introduction

To achieve green and low-carbon development in energy, the Chinese government has put forward the development strategy of "carbon peak and carbon neutrality", and the electrical power industry has continuously adjusted its energy structure (Yang et al., 2022). A large number of uncertain and fluctuating renewable energy power, which mainly includes solar energy and wind energy, has been connected to the power grid (Wang et al., 2023a). Currently, it is impractical and expensive to build large-scale energy storage to absorb the impact of the intermittent, strong fluctuations in the power supply of renewable energy to the grid. Thus, the load regulation capacity of thermal power units in response to automatic generation control (AGC) directly affects the power grid regulation security. Due to the need for deep peak shaving conditions, the power grid has put forward higher requirements for

the coordinated control ability of thermal power plants (Wang et al., 2023b). Therefore, the accurate prediction and improvement of the AGC regulation capability of thermal power plants is of great significance for ensuring the safe operation of the power grid system (Li et al., 2023; Zhou et al., 2023).

To encourage thermal power plants to improve regulatory flexibility and AGC regulation capability, the Chinese National Energy Administration laid down the rules suitable for grid-connected entities involving power dispatching, that is, "management rules of grid-connected operation of power plant in Northern China" and "management rules of auxiliary service of the grid-connected power plant in Northern China" (i.e., "two rules"). The "two rules" clarifies the calculation method of the regulation capability index $K_p$ of thermal power plants and the profit value under different capabilities. The AGC regulation capability of coal-fired thermal power plants are closely related to the coordinated control system of the units (Peng et al., 2023). Ref (Eslick et al., 2022) develops a physics-based coordinated control system model to improve load-following performance and optimize other boiler operating variables of a 245 MW subcritical pulverized coal-fired power plant. In Ref. (Liu et al., 2022), conventional AGC strategies were proposed to calculate the total adjustment power based on the information collected from Supervisory Control and Data Acquisition system including frequency deviation, tie-line power deviation, and area control error (ACE); however, the field test process is usually tedious and may bring influence to the normal power generation process. Wang et al. (Wang J. et al., 2019) proposed an AGC performance evaluation method by comparing the magnitude change of the generated power and the desired power, which is more convenient than the field test process. However, this method failed to consider the dynamic characteristics of the unit and the influence of noise, and its accuracy needs to be improved. Egido et al. (Egido et al., 2007) proposed using operational data analysis to evaluate AGC performance, in which the dynamic characteristics of the unit were considered, thereby improving the accuracy of the evaluation results. Wang et al. (Wang et al., 2017) applied genetic algorithms to optimize the controller parameters of the AGC assessment index to improve the AGC performance index of thermal power units.

Considering the uncertainty and non-linearity of the process characteristics of thermal power plants, researchers have constructed neural network models to predict the regulation capability of responding to the AGC instruction from the power grid. For example, Chen et al. (Chen and Wang, 2016) proposed a neural network-based predictive control algorithm to handle nonlinear problems in the AGC response. Xi et al. (Xi et al., 2020) proposed a novel DPDPN algorithm to improve AGC power allocation, and the predictive capability of deep learning was combined with the decision-making ability of reinforcement learning in the DPDPN method. Peng et al. (Peng et al., 2019) combined the optimization strategy of traditional predictive control with a neural network and proposed a new system-fitting algorithm based on the Bayesian neural network; however, it failed to consider the screening of variables and features, which led to long training time of the network and inadequate prediction accuracy. Wang et al. (Wang et al., 2021) utilized a long short-term memory neural network (LSTM) model to evaluate the performance of thermal power plants, and the prediction results were more accurate and

stable, but they did not consider the feature selection problem in the model construction. To solve this problem, Ref (Liang et al., 2019) proposed a max-relevance and min-redundancy (mRMR) algorithm for feature extraction, thereby improving the model training efficiency. Therefore, in this paper, the AGC influencing factors are analyzed and extracted by using the mRMR algorithm, and the obtained variables are then taken as the inputs to the LSTM model to predict the AGC regulation capability of the power plant.

At present, the common approaches to improve the power generation change rate of thermal power units can include condensate throttling, steam extraction of heating units, refrigerant throttling of condensers, etc. (Hegazy et al., 2016; Zhang et al., 2021; Liu et al., 2023). These methods can greatly improve the dynamic characteristics of thermal power plants, shorten the response time of units, and increase the primary and secondary frequency regulation capabilities through rational utilization of turbine-side energy storage. For example, the condensate throttling control mainly uses the working medium storage capacity provided by the condensate water tank and the deaerator tank; thus, the energy originally used for heating the feed water in the reheating system can be temporarily utilized to increase the variable load rate of the unit.

It can be found that by changing the energy storage on the turbine side, the main steam temperature and pressure of the power plant can be quickly adjusted, thus improving the load change rate, that is, the regulation capability to AGC instruction. The main steam temperature and pressure of the turbine are ultimately affected by boiler side parameters, such as the coal feed rate, air supply rate, and feedwater flow rate (Stevanovic et al., 2018; Wang Y. et al., 2019; Yin et al., 2022). Therefore, this paper considers the construction of multi-stage sub-models to describe the AGC regulation capability. In the first sub-model, historical sequences of parameters such as coal feed rate, air supply rate, and feedwater flow rate are taken as inputs of an LSTM model; the main steam temperature and main steam pressure are taken as output parameters to be predicted. In the second sub-model, the prediction of the main steam temperature and main steam pressure are taken as inputs of another LSTM model, and the final power load change, that is, the actual power generation, is taken as output. Based on the constructed model, the particle swarm optimization (PSO) algorithm is proposed to optimize parameters of coal feed rate, air supply rate, and feedwater flow rate, to improve the AGC regulation capacity.

The rest of this paper is organized as follows. Section 2 details the fundamental modeling theories. The AGC regulation capacity model and optimization methods are presented in Section 3. Section 4 gives an application to a 300 MW thermal power plant, and Section 5 provides the conclusions.

# 2 Modeling theories

## 2.1 mRMR feature selection

The max-relevance and min-redundancy (mRMR) is a filtering feature selection algorithm, in which the evaluation function considers both the correlation between features and categories and the correlation between features. As a result, the filtered variables can retain the maximum number of relevant features
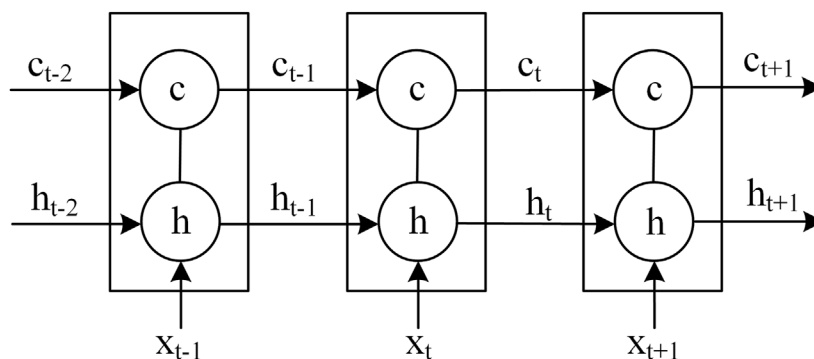
**FIGURE 1**
LSTM neural network structure diagram.

while ensuring the minimum number (R et al., 2016; Ding and Peng, 2003). The algorithm uses mutual information to measure the correlation between variables, which can be expressed as follows:

$$I(\boldsymbol{M};\boldsymbol{N}) = \iint p(m,n)log\left(\frac{p(m,n)}{p(m)p(n)}\right)dmdn \qquad (1)$$

where $\boldsymbol{M}$ and $\boldsymbol{N}$ are two characteristic variables, $p(m)$ and $p(n)$ are marginal probability functions of the corresponding variables, and $p(m,n)$ is the joint probability distribution.

Given a subset of candidate features, the measures for maximum correlation between features and categories and minimum redundancy between features are calculated as follows:

$$\max D(\boldsymbol{S},c), D = \frac{1}{|\boldsymbol{S}|} \sum_{f_i \in S} \boldsymbol{I}(f_i, c) \qquad (2)$$

$$\min R(\boldsymbol{S},c), R = \frac{1}{|\boldsymbol{S}|^2} \sum_{f_i,f_j \in S} \boldsymbol{I}(f_i, f_j) \qquad (3)$$

where $\boldsymbol{S}$ is the set of features, $f_i$ is the $i$-th feature, $c$ is the target category, $\boldsymbol{I}(f_i, c)$ is the mutual information between feature $i$ and target category $c$, $\boldsymbol{I}(f_i, f_j)$ is the mutual information between feature $i$ and feature $j$, $D$ is the measure with the greatest correlation between features and categories, and $R$ is the measure with the least redundancy between two different features.

Considering the relevance and redundancy of the selected feature subset, the evaluation function of the mRMR feature selection is obtained by combining Eqs. 2, 3, which is given as follows:

$$\max J(D,R), J = D - R \qquad (4)$$

The above equation can be solved by gradually increasing a single variable. Assuming that the set $\boldsymbol{S}$ is the full feature set, and $\boldsymbol{S}_{t-1}$ is the already selected feature set with $t-1$ features, then the $t$-th feature is selected from the set $\boldsymbol{S}$, which is different from the elements in the set $\boldsymbol{S}_{t-1}$, to maximize Eq. 4. In other words, we can use Eq. 5 to maximize the differences between univariate relevance and redundancy to determine the added $t$-th feature (Wang et al., 2018).

$$\max_{f_i \in S-S_{t-1}} \left[ \boldsymbol{I}(f_i, c) - \frac{1}{t-1} \sum_{f_i \in S_{t-1}} \boldsymbol{I}(f_i, f_j) \right] \qquad (5)$$

## 2.2 LSTM neural network

Long short-term memory neural network is one variant of a Recurrent Neural Network (RNN). An LSTM neural network has a temporal recurrent neural network structure designed to solve the problems of gradient disappearance and gradient explosion RNN when processing long sequence data (Hochreiter and Schmidhuber, 1997). A typical LSTM model mainly consists of one input layer, one output layer, and several hidden layers. The implicit layer has three types of gate structures with a memory unit, which is responsible for storing state information and passing it forward. The three types of gates are the forgetting gate, the input gate, and the output gate (Sahin and Kozat, 2019; Yu et al., 2019; Yuan et al., 2019). The structure of the LSTM neural network is shown in Figure 1.

It is shown in Figure 1 that each LSTM has a cell, which can be regarded as the memory unit of the LSTM. At the time $t$, there are three inputs: the input value of the current moment memory unit $x_t$, the output value of the previous moment memory unit $h_{t-1}$, the memory unit state of the previous moment $c_{t-1}$; and two outputs: the output value of the current moment memory unit $h_t$, the current moment memory unit state $c_t$.

LSTM can get and modify the information in each memory unit through the input gate $i_t$, output gate $o_t$ and forget gate $f_t$. The forget gate determines how much of the unit state $c_{t-1}$ at the previous moment is retained until the current moment. The input gate determines the information of input $x_t$ saved to the cell state at the current moment. The output gate controls the information from the current output value of the LSTM $c_t$ to the cell state $h_t$. The relation among all the variables can be calculated as follows:

$$\begin{aligned} i_t &= \sigma(\boldsymbol{w}_i[\boldsymbol{h}_{t-1}, \boldsymbol{x}_t] + b_i) \\ o_t &= \sigma(\boldsymbol{w}_o[\boldsymbol{h}_{t-1}, \boldsymbol{x}_t] + b_o) \\ f_t &= \sigma(\boldsymbol{w}_f[\boldsymbol{h}_{t-1}, \boldsymbol{x}_t] + b_f) \end{aligned} \qquad (6)$$

where $\boldsymbol{w}$ is the weight matrix, $\boldsymbol{b}$ is the corresponding bias term, which can be obtained by the network training self-learning optimization, and $\boldsymbol{\sigma}$ is the activation function sigmoid function, with the output value ranging from 0 to 1.

LSTM layer can calculate unit status updates at this time value $\tilde{c}_t$ according to the last moment of the network output and the current time of input; furthermore, the current state of unit $c_t$ can be
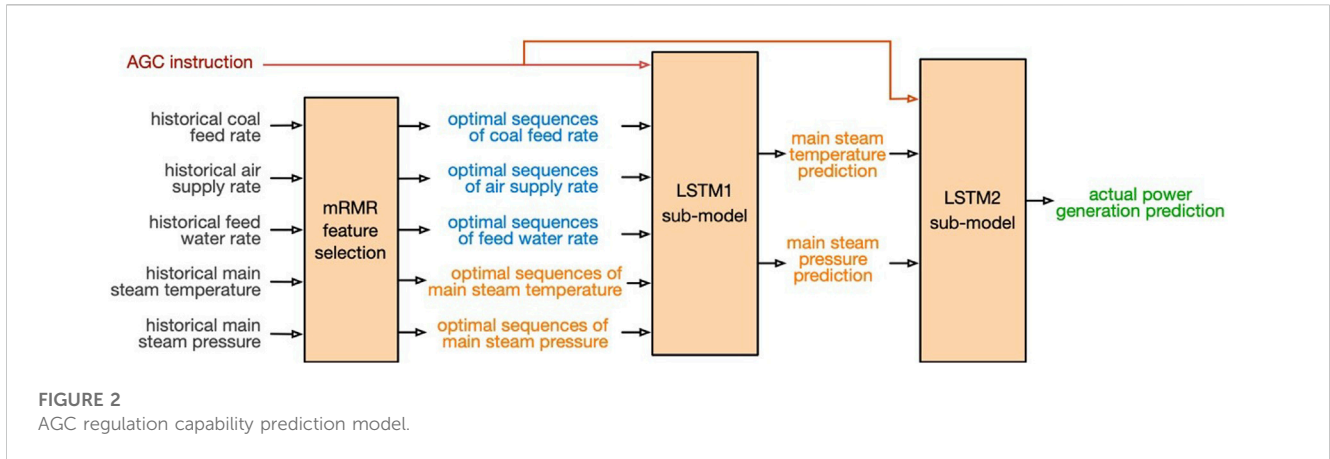
**FIGURE 2**
AGC regulation capability prediction model.

calculated based on the forgotten gate and input, which is shown as follows:

$$\tilde{c}_t = tanh\left(w_c\left[h_{t-1}, x_t\right] + b_c\right)$$
$$c_t = f_t c_{t-1} + i_t \tilde{c}_t \qquad (7)$$

The cell state has two flow directions. One direction is to pass the LSTM layer at the next moment in the feedback structure as a long-term information feature; the other is to combine with the *tanh* function and multiply with the result of the output gate to obtain the predicted result of the current moment, that is, $h_t = o_t \odot tanh\left(c_t\right)$, where $h_t$ is the final output of the network, $\odot$ refers to the Hadamard product.

# 3 AGC regulation capacity model and optimization

## 3.1 Model structure

The structure of the AGC regulation capability model is shown in Figure 2. The whole model contains multi sub-models, one of which is the prediction model of boiler performance, and the other is the prediction model of the actual generation power of the generator. In the first sub-model, historical sequences of coal feed rate, air supply rate, feedwater flow rate, main steam pressure, and main steam temperature are taken as the model input; the main steam pressure and main steam temperature value at the next sampling period are taken as the model output, to characterize the response of the boiler to the AGC instruction from the power grid. In the second sub-model, the main steam temperature and pressure predicted by the first sub-model are taken as the input, and the actual generating power is taken as the output.

When the AGC instruction is given, the main steam pressure and main steam temperature response process are related to their historical values; therefore, historical values of the coal feed rate, air supply rate, and feedwater flow rate are utilized as the input of the first sub-model. The prediction process is shown in Eq. 8.

$$\hat{p}_{k+1} = f_1\left(P_{ek}, c_k, c_{k-1}, \cdots, c_{k-T}, a_k, a_{k-1}, \cdots, a_{k-T}, w_k, w_{k-1}, \cdots, w_{k-T},\right.$$
$$\left. p_k, p_{k-1}, \cdots, p_{k-T-1}, t_k, t_{k-1}, \cdots, t_{k-T}\right)$$

$$\hat{t}_{k+1} = f_2\left(P_{ek}, c_k, c_{k-1}, \cdots, c_{k-T}, a_k, a_{k-1}, \cdots, a_{k-T}, w_k, w_{k-1}, \cdots, w_{k-T},\right.$$
$$\left. p_k, p_{k-1}, \cdots, p_{k-T-1}, t_k, t_{k-1}, \cdots, t_{k-T}\right) \qquad (8)$$

where $k$ is the current time stamp, $T$ is the maximum historical time to be used ($T \geq 1$), $P_{ek}$ is the current value of the AGC instruction received from the power grid, $c_{k-i}, a_{k-i}, w_{k-i}$ ($1 \leq i \leq T$) represent the $i$ th historical value of the coal feed rate, air supply rate, and feedwater flow rate, $c_k, a_k, w_k$ represent the value of the coal feed rate, air supply rate, and feedwater flow rate to be set; $\hat{p}_{k+1}$ and $\hat{t}_{k+1}$ represent the predicted value of the main steam pressure and main steam temperature at next time stamp.

Definitely, the parameters of $\hat{p}_{k+1}$ and $\hat{t}_{k+1}$ to be predicted are closely related to the current values of $c_k, a_k, w_k, p_k$, and $t_k$. As to the historical sequence of $c_{k-1}, \cdots, c_{k-T}$, $a_{k-1}, \cdots, a_{k-T}$, $w_{k-1}, \cdots, w_{k-T}$, $p_{k-1}, \cdots, p_{k-T-1}$, and $t_{k-1}, t_{k-2}, \cdots, t_{k-T}$, not all historical sequence values are used as model inputs. The optimal set of these parameters can be determined by the mRMR method.

The actual power generation of a thermal power plant is closely related to the main steam pressure and main steam temperature according to the operation mechanism of the steam turbine. Therefore, the actual power generation can be obtained based on the prediction of the main steam pressure and main steam temperature. That is, the AGC instruction value, the main steam pressure, and the main steam temperature are used as input variables of the LSTM network in the second sub-model to predict the final actual power generation. The prediction process is shown in Eq. 9.

$$\hat{P}_{k+1} = f_3\left(P_{ek}, \hat{p}_{k+1}, p_k, \hat{t}_{k+1}, t_k\right) \qquad (9)$$

where $\hat{p}_{k+1}$ and $\hat{t}_{k+1}$ represent the main steam pressure and main steam temperature predicted by the first sub-model, $\hat{P}_{k+1}$ is the prediction of actual power generation, which can characterize the regulation capability to the AGC instruction of the power grid.

## 3.2 AGC regulation capability optimization

According to the AGC regulation mechanism, the boiler and turbine will be tuned through the coordinated control system when the thermal power plant receives the AGC instruction. The final response of the plant is determined by the operating parameters of the coal feed rate, air supply rate, and feedwater flow rate. Therefore,
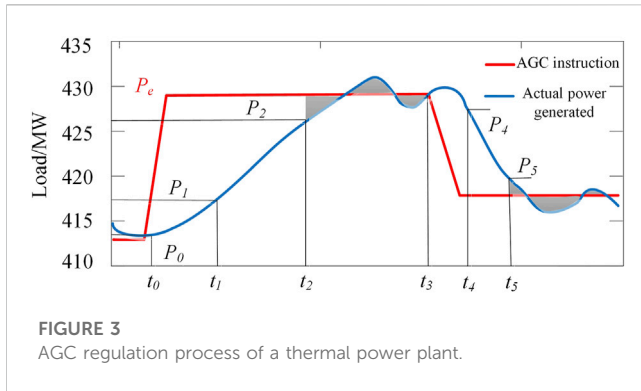
FIGURE 3
AGC regulation process of a thermal power plant.

these parameters can be optimized to maximize the regulation capability for a given AGC instruction.

According to the management rules of grid-connected operation of power plants, the regulation capability index is calculated by the $K_p$ after the actual generated power is obtained by using multi sub-models shown in Eqs. 8, 9.

To illustrate the calculation of $K_p$, an AGC regulation process is considered, for example,. Figure 3 shows the curve of an actual power generation (i.e., power load) responding to a given AGC instruction, with a dead zone of 1% and a regulation dead zone of 0.5% of the unit-rated capacity. The response time from $P_0$ to $P_1$ in Figure 3 and the calculation is as follows:

$$t = t_1 - t_0 \tag{10}$$

The regulation rate refers that the output crosses the response dead zone to enter the regulation dead zone. In Figure 3, the regulation rate can be calculated in $t_1 \sim t_2$ or $t_3 \sim t_4$ period. Taking load increasing process ($t_1 \sim t_2$ period) as an example (same results can be obtained in the load decreasing process, i.e., $t_3 \sim t_4$ period), the calculation formula is as follows:

$$v = \frac{P_2 - P_1}{t_2 - t_1} \tag{11}$$

The regulation accuracy refers to the integration of the absolute value of the difference between the actual output and the set point command over a while (the result is shown in the shaded part in Figure 3), and then it is divided the integrated value by the integration time, which is the regulation accuracy for that period. The calculation is given as follows:

$$\Delta_p = \frac{\int_{t_2}^{t_3} |P(t) - P_e| dt}{t_3 - t_2} \tag{12}$$

where $\Delta_p$ is the regulation accuracy, $P(t)$ is the actual output of the power plant, and $P_e$ is the AGC instruction received from the power grid.

According to the "two rules", the regulation capability index is calculated by the $K_p$ after the actual power generation is obtained. The detailed calculation equations are given as follows.

$$K_p = K_1 \cdot K_2 \cdot K_3 \tag{13}$$

where,

$$K_1 = 2 - v_N / v \tag{14}$$

$$K_2 = 2 - \Delta_p / \Delta_{p_N} \tag{15}$$

$$K_3 = 2 - t / t_N \tag{16}$$

where $v_N$, $\Delta_{p_N}$, and $t_N$ are intrinsic parameters of the investigated power plant, and they refer to the standard value of regulation speed, allowable deviation, and response time, respectively.

The task of regulation capability improvement is to maximize the index of $K_p$ value when an AGC instruction is received from the power grid by optimizing the operating parameters, including the coal feed rate $c_k$, air supply rate $a_k$, and feedwater flow rate $w_k$. However, the index $K_p$ can only be calculated after the whole AGC response process is finished. If the index $K_p$ is directly used as the objective function, the online optimization cannot be realized, because the $K_p$ index cannot be obtained at each time stamp. From Eqs 10–16, it can be found that if the actual power generation of the unit is closer to the AGC instruction, the $K_p$ index will be larger. Therefore, the minimization of the difference between the actual power generation and AGC instruction can be considered as the objective function.

In addition, according to the secure operation of thermal power plants, the following constraints are considered. For a given 300 MW thermal power plant, the upper and lower operation limits of the main steam pressure are set to 22.7 MPa and 17.2 MPa, respectively; the upper and lower limits of the main steam temperature are set to 569°C and 559°C, respectively. The fluctuation limit of the main steam pressure per second is less than 0.5 MPa. The upper limit of the unit load is 300 MW while the lower limit is 128 MW. Then we can obtain the following optimization problem:

$$\min_{c_k, a_k, w_k} \frac{1}{2} \left\| \hat{P}_{k+1} - P_{e_k} \right\|^2$$

$$\text{s.t.} \begin{cases} \left| \hat{p}_{k+1} - p_k \right| < 0.5 \, MPa \\ 15.5 \, MPa < \hat{p}_{k+1} < 18.2 \, MPa \\ 559 \, ℃ < \hat{t}_{k+1} < 569 \, ℃ \\ 128 \, MW < \hat{P}_{k+1} < 300 \, MW \end{cases} \tag{17}$$

The particle swarm optimization (PSO) algorithm is utilized here to obtain the optimal operating variables. These variables are regarded as particles in multi-dimensional search space, and the moving speed and direction of the particles are updated by iterating to obtain the optimal solution (Zhang et al., 2015; Liu et al., 2020). The variable to be optimized is denoted as $x = [c_k, a_k, w_k]^T$, and a particle population is generated in the search space:

$$\begin{cases} x_i = \{x_1, x_2, \cdots, x_m\} \\ v_i = \{v_1, v_2, \cdots, v_m\} \end{cases} \tag{18}$$

where $x_i$ and $v_i$ are the position and velocity of the $i$ th particle, respectively, and $m = 3$ represents the variable dimension.

For the $i$ th particle at the $t$ th iteration, the velocity and position are denoted as $x_i^t$ and $v_i^t$, respectively, and the individual optimal value and the global optimal value are $p_{best}^t$ and $g_{best}$. The particle updates its velocity and position information according to Eqs. 19 and (20) in $(t + 1)$ th iteration:

$$v_i^{t+1} = \omega v_i^t + c_1 r \left( p_{best}^t - x_i^t \right) + c_2 r \left( g_{best} - x_i^t \right) \tag{19}$$
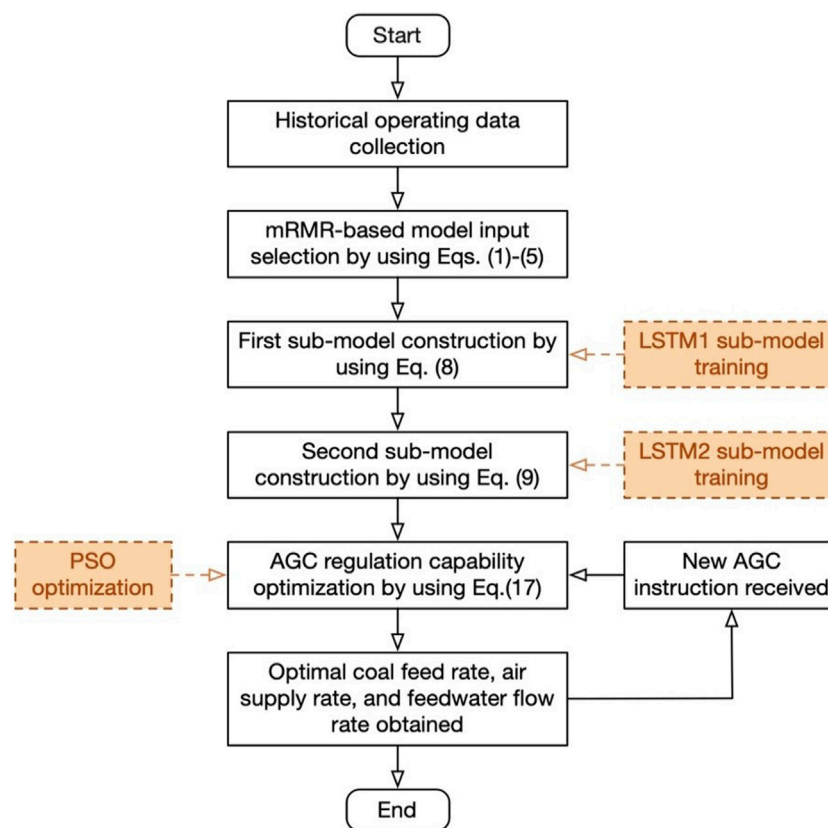
$$x_i^{t+1} = x_i^t + v_i^{t+1} \tag{20}$$

**FIGURE 4**
Flowchart of the AGC regulation modeling and optimization.

where $\omega, c_1, c_2$ are the weight and learning factors of particles during velocity update, $r$ represents a random number from 0 to 1.

With Eq. 17 as the fitness function, the speed and position of the particles are updated according to Eqs 19, 20. The best solution $x$ corresponds to the optimal values of $[c_k, a_k, w_k]^T$ to be set.

## 3.3 Model implementation procedure

The implementation process of the AGC regulation modeling and optimization is shown in Figure 4, and the specific steps are given as follows:

(1) Collect historical operating data of the power plant in several periods of the AGC regulation process, including the parameters of coal feed rate, air supply rate, feedwater flow rate, the main steam pressure, and main steam temperature.
(2) Calculate mutual information between input and output variables, and select the optimal historical sequences of coal feed rate, air supply rate and feedwater flow rate as the inputs of the first sub-model.
(3) Construct the first sub-model with the extracted parameters in (2) as the inputs, to predict the main steam pressure and main steam temperature at the next time stamp by using the LSTM network.

(4) Construct the second sub-model, with the outputs of the first sub-model in (3) as the inputs, to predict the actual power generation at the next time stamp by using LSTM network.
(5) Given a new AGC instruction, optimize the values of coal feed rate, air supply rate, and feedwater flow rate by minimizing the difference between the actual power generation and AGC instruction.
(6) Obtain the optimal coal feed rate, air supply rate, feedwater flow rate and go to (5) to get a new AGC instruction.

# 4 Application analysis

## 4.1 Data acquisition

In this paper, we obtain a high-resolution operation data set from the DCS system of a 300 MW coal-fired subcritical unit in North China. The unit is equipped with a subcritical parameter natural circulation steam package boiler with a maximum continuous output of 1,016 t/h. AGC regulation experiments were conducted to collect operation data containing the parameters shown in Table 1. The data samples were acquired with an interval of one second, with a total of 3,600 samples obtained. The AGC regulation curve is shown in Figure 5, including load-raising or decreasing processes.
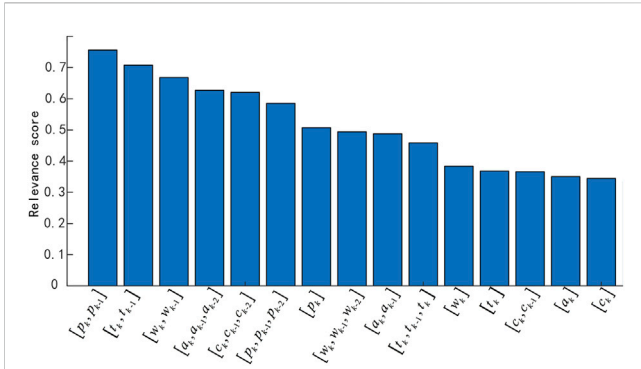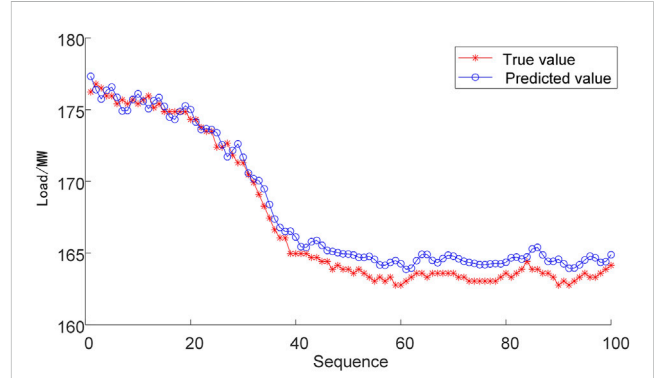
**FIGURE 5**
Ranking of variable relevance scores.



**FIGURE 6**
The mRMR-mLSTM model prediction.

**TABLE 1 Range of parameters.**

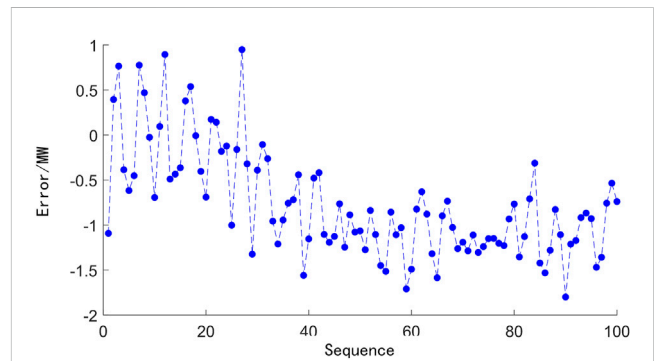| Number | Features | Range | Unit |
|--------|----------|-------|------|
| 1 | Actual power generation | 164.42–233.87 | MW |
| 2 | AGC instruction | 162.78–234.75 | MW |
| 3 | Main steam temperature | 563.69–578.94 | ℃ |
| 4 | Main steam pressure | 15.65–19.37 | MPa |
| 5 | Coal feed rate | 94.05–140.66 | t/h |
| 6 | Air supply rate | 758.60–935.87 | t/h |
| 7 | Feedwater flow rate | 498.92–720.29 | t/h |



**FIGURE 7**
The mRMR-mLSTM model prediction error.

The data samples were preprocessed by using the z-score normalization to make them conform to a standard normal distribution, that is, with a mean of 0 and a standard deviation of 1. We use the above data to construct a LSTM model to achieve the prediction of unit power generation and the validation of unit AGC capability optimization strategy. The first 3,000 sets of collected data are used as the training set, and the last 600 sets of data are used as the test set to verify the training and optimization results of the model. Because the input data of the LSTM model is sequence data, the training set and test set data were divided into 43 and 10 sequence data based on AGC instructions' changing.

## 4.2 Model accuracy analysis

The mRMR was used to extract the feature variables, and the correlation score of each variable was calculated comprehensively, as shown in Figure 5. The characteristic variables with correlation scores greater than 0.5 were selected as input variables. Therefore, the maximum historical time $T$ of the coal feed rate, air supply rate, and feedwater flow rate were set to 3, 3, and 2, respectively; the maximum historical time $T$ of the main steam pressure and main steam temperature are both set to 2.

The first sub-model of the LSTM network is set up to predict the main steam pressure and the main steam flow, respectively. The

second sub-model of the LSTM network was used to predict the final actual power generation. Taking one sequence data containing 100 samples in the test set data as an example, the prediction results are shown in Figure 6, where the predicted and actual curves of the model nearly coincide. Figure 7 shows the model prediction error between the actual power generation and the model prediction is within 1.81 MW, which validates the accuracy of the proposed model.

The average relative error (ARE), root mean square error (RMSE), and normalized root mean square error (NRMSE) were used as indexes to qualitatively evaluate the accuracy of the model, and each index was defined as follows:

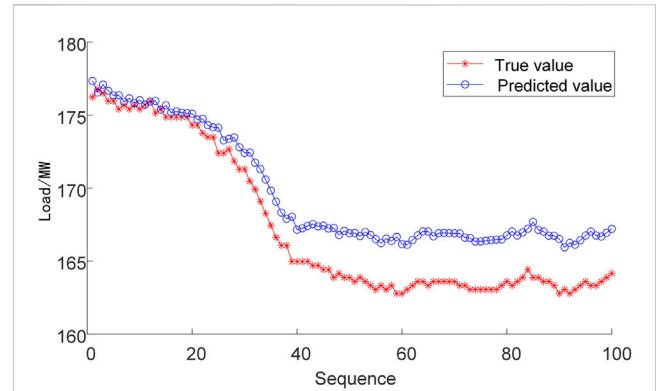$$ARE = \frac{1}{n}\sum_{i=1}^{n}\frac{\left|\hat{P}_i - P_i\right|}{P_{max} - P_{min}} \times 100\% \qquad (21)$$

$$RMSE = \sqrt{\frac{1}{n}\sum_{i=1}^{n}\left(\hat{P}_i - P_i\right)^2} \qquad (22)$$

$$NRMSE = \frac{1}{\bar{P}}\sqrt{\frac{1}{n}\sum_{i=1}^{n}\left(\hat{P}_i - P_i\right)^2} \times 100\% \qquad (23)$$
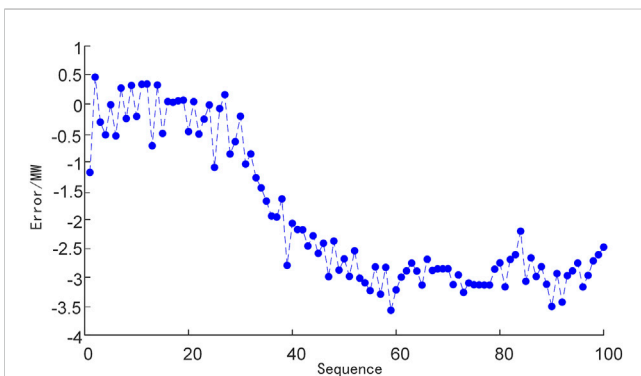
where $P_i$, $\hat{P}_i$ represents the actual and predicted value of the power generation, $\bar{P}$ represents the mean value of actual power generation, $P_{max}$ and $P_{min}$ represent the maximum and minimum values of $P_i$,
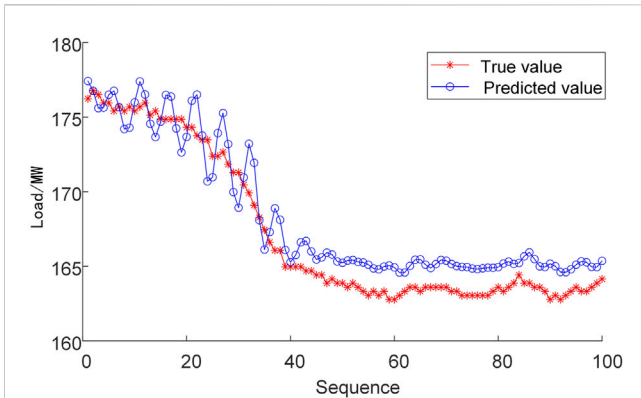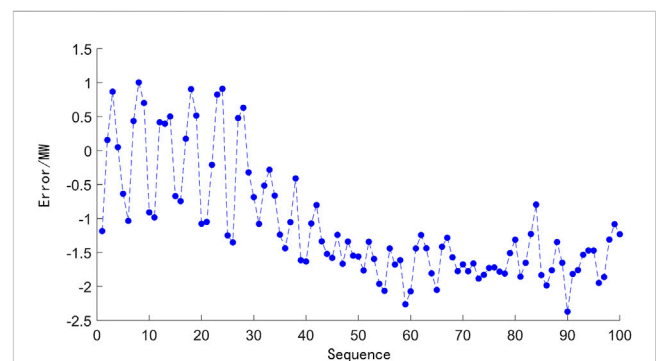
FIGURE 8
The mLSTM model prediction result.



FIGURE 10
The LSTM model prediction result.



FIGURE 9
The mLSTM model prediction error.



FIGURE 11
The LSTM model prediction error.

and $n$ is the sample number. The ARE, RMSE, and NRMSE of the model on the test sets are 9.4%, 1.53 MW, and 0.97%, respectively. The results showed that the error of the proposed model was adequate to give an accurate prediction of actual power generation with a given AGC instruction.

To further verify the prediction performance of the proposed model with multi sub-LSTMs and mRMR-based feature selection (denoted as mRMR-mLSTM model), the model was compared with a single LSTM neural network model (denoted as LSTM model), and a model with multi sub-LSTMs and no mRMR-based feature selection (denoted as mLSTM model). The comparison of model prediction results and errors is shown in Figures 8–11. It can be seen that the predicted power generation of the single LSTM neural network model differs significantly from the actual power generation with a given AGC instruction, and the peak value of the model prediction errors reaches 3.94 MW. The mLSTM model has improved the accuracy compared with the single LSTM network, but the error is still larger than that of the mRMR-mLSTM model.

The comparison results of the single LSTM model, the mLSTM model, and the mRMR-mLSTM model are given in Table 2. The results showed that the error of the mRMR-mLSTM model was significantly lower than that of the LSTM model and the mLSTM model. Specifically, compared with the

single LSTM model, the prediction RMSE error of the mLSTM model is reduced by 1.15 MW, with a 35.1% decrease, and the results show that it conforms to the real responding characteristics better by dividing the AGC process into multi-stages, which are described by different sub-models. In addition, the prediction RMSE error of the proposed mRMR-mLSTM model is less than 1.74 MW and reduced by 53.2% compared with the single LSTM model, which means the feature selection based on mRMR is beneficial to filter the relevant variables related to the AGC response. In general, the proposed mRMR-mLSTM model can be adequate to give an accurate prediction of actual power generation with a given AGC instruction.

## 4.3 AGC capability optimization results

Figure 12 shows the variation trend of the actual power generation of the thermal power plant in response to the AGC instruction. It can be seen that when the power plant receives the AGC instruction from the power grid, the values of the coal feed rate, air supply rate, and feedwater flow rate start to vary, and then the main steam pressure and main steam temperature also change at the same time, which results to the change of the actual power generation. Finally, the actual power generation reaches around
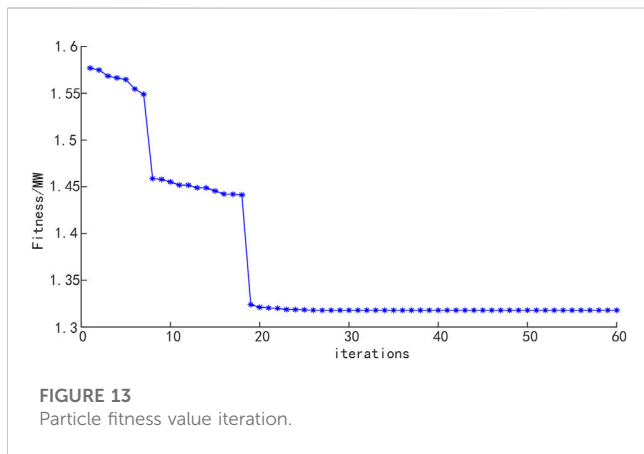
**TABLE 2 Prediction accuracy comparison of different models.**

| Models | Test sets | | |
|---|---|---|---|
| | ARE/% | RMSE/MW | NRMSE/% |
| LSTM | 16.8 | 3.27 | 1.9 |
| mLSTM | 13.3 | 2.12 | 1.2 |
| mRMR-mLSTM | 9.4 | 1.53 | 0.97 |
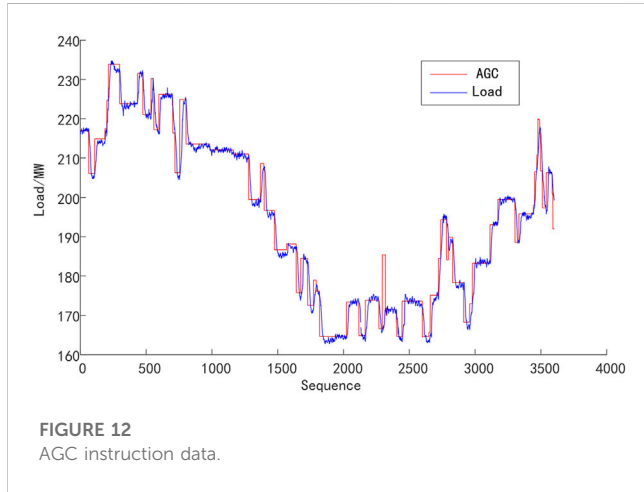


FIGURE 12
AGC instruction data.



FIGURE 13
Particle fitness value iteration.

the AGC command value. In addition, we can use Eqs 10–16 to calculate the $K_p$ value for the entire response.

With the error between the actual power generation and AGC instruction as the objective function, PSO is used to obtain the optimal values of the coal feed rate, air supply rate, and feedwater flow rate. Taking the optimization of the first time stamp as an example, the iterative process of PSO is shown in Figure 13. It can be seen that after 19 iterations, the objective function achieves the optimal value, and the deviation reaches 0.18 MW. Similarly, the optimization can be conducted online and we can get the optimal coal feed rate, air supply rate, and feedwater flow rate at each moment during the AGC regulation process. Correspondingly, the actual power generation can be obtained by using Eq. 9, which is shown in Figure 14.
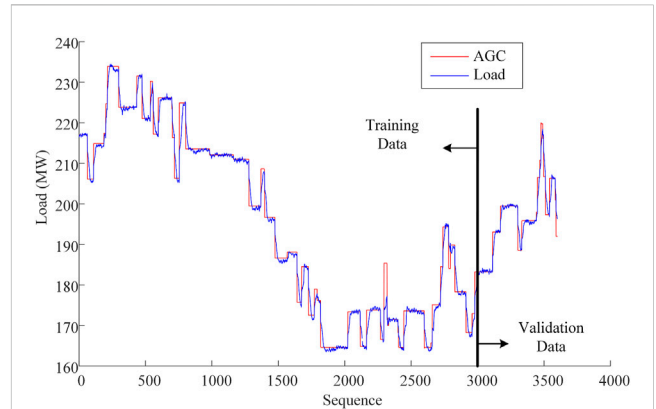


FIGURE 14
Actual power generation after optimization and AGC instruction.
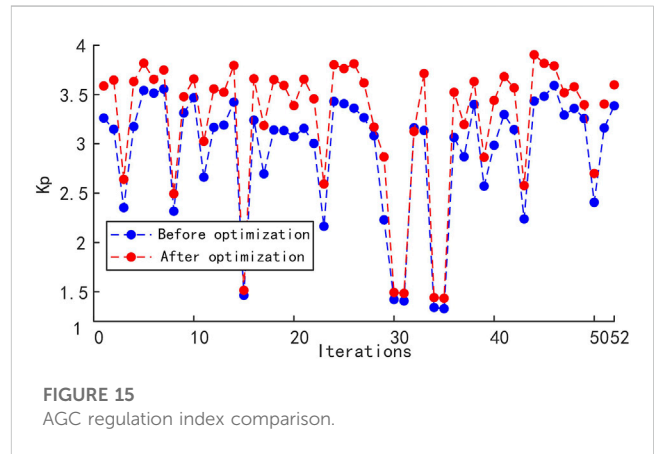


FIGURE 15
AGC regulation index comparison.

As illustrated in Section 4.2, the LSTM model can give accurate predictions, which means the model is adequate to represent the actual operating characteristics of coal-fired unit. Thus, we consider it may be reasonable to use the calculation results for the comparison. During the experiment, the investigated power plant receives 52 AGC instructions from the power grid, and most of instructions maintain for approximately 1–2 min. According to the AGC instruction and actual power generation, the $K_p$ index can be calculated in each AGC regulation process by using Eqs. 10)-16. The $K_p$ index of the AGC regulation before and after PSO optimization is shown in Figure 15. It is easily obtained that the average $K_p$ value of the AGC regulation before the optimization is only 2.98, and its value increases to 3.448 after optimizing the coal feed rate, air supply rate, and feedwater flow rate by using PSO, with a 15.7% improvement. Thus, it can be concluded that the proposed method can effectively improve the AGC regulation capability of the thermal power plant.

# 5 Conclusion

This paper proposes a prediction and optimization model for the AGC regulation capacity of thermal power units. Firstly,

optimal historical sequences of the coal feed rate, air supply rate, feedwater flow rate, main steam temperature, and pressure are selected by using mRMR theory and are taken as the first sub-model of LSTM to predict the future values of main steam temperature and pressure, which are then considered as the inputs of the second LSTM sub-model to predict the power generation with a given AGC instruction. Then, based on the model, the PSO is applied to obtain optimal values of the coal feed rate, air supply rate, and feedwater flow rate by minimizing the difference between the actual power generation and AGC instruction. Finally, an application to a 300 MW power plant AGC regulation process is conducted. Comparisons results of different modeling methods show that the proposed mRMR-mLSTM model is adequate to predict the AGC regulation capability after introducing the mRMR feature selection and multi-stage process modeling, and the prediction RMSE error is 1.53 MW, which is reduced by 53.2% compared with the single LSTM model. In addition, after optimization by PSO, the AGC regulation index Kp reaches 3.448, which is improved by 15.7%. Thus, the proposed method can effectively predict and improve the adjustment capability of grid AGC recommendation.

## Data availability statement

The data analyzed in this study is subject to the following licenses/restrictions: The dataset of this article was collected from a 300 MW coal-fired unit. Requests to access these datasets should be directed to 19072318559@163.com.

## Author contributions

FJ: Writing–original draft. XH: Writing–original draft. WZ: Writing–original draft. MW: Writing–original draft. BW: Writing–original draft.

## Funding

## Conflict of interest

Authors FJ, XH, WZ, MW, and BW were employed by State Grid Hebei Energy Technology Service Co Ltd.

## Publisher's note

All claims expressed in this article are solely those of the authors and do not necessarily represent those of their affiliated organizations, or those of the publisher, the editors and the reviewers. Any product that may be evaluated in this article, or claim that may be made by its manufacturer, is not guaranteed or endorsed by the publisher.

## References

Chen, D., and Wang, L. (2016). "Neural network based predictive automatic generation control," in Proceedings of the IEEE Power and Energy Society General Meeting, IEEE Computer Society, Boston, MA, United states, July, 2016. doi:10.1109/PESGM.2016.7741573

Ding, C., and Peng, H. (2003). "Minimum redundancy feature selection from microarray gene expression data," in Proceedings of the 2003 IEEE Bioinformatics Conference, Institute of Electrical and Electronics Engineers Inc., Stanford, CA, United states, August, 2003, 523–528. doi:10.1109/CSB.2003.1227396

Egido, I., Fernández-Bernal, F., and Rouco, L. (2007). Evaluation of Automatic Generation Control (AGC) regulators by performance indices using data from real operation. Transm. &amp 1 (2), 294–302. doi:10.1049/iet-gtd:20060173

Eslick, J. C., Zamarripa, Miguel, A., Ma, J., Bhattacharya, I., Rychener, B., et al. (2022). Predictive modeling of a subcritical pulverized-coal power plant for optimization: parameter estimation, validation, and application. Appl. Energy 319, 119226. doi:10.1016/j.apenergy.2022.119226

Hegazy, A., Rothan, Y., and Engeda, A. (2016). Feasibility of using vapor compression refrigeration system for cooling steam plant condenser. Appl. Therm. Eng. 106 (5), 570–578. doi:10.1016/j.applthermaleng.2016.06.005

Hochreiter, S., and Schmidhuber, J. (1997). Long short-term memory. Neural Comput. 9 (8), 1735–1780. doi:10.1162/neco.1997.9.8.1735

Kennedy, J., and Eberhart, R. (1995). "Particle swarm optimization," in Proceedings of the IEEE International Conference on Neural Networks, Piscataway, NJ, USA, November, 1995, 1942–1948. doi:10.1109/ICNN.1995.488968

Li, B., Wang, S., Li, B. T., Li, H. B., and Wu, J. Z. (2023). Optimal performance evaluation of thermal AGC units based on multi-dimensional feature analysis. Appl. Energy 339, 120994. doi:10.1016/j.apenergy.2023.120994

Liang, Y., Niu, D., and Hong, W. (2019). Short term load forecasting based on feature extraction and improved general regression neural network model. Energy 166 (1), 653–663. doi:10.1016/j.energy.2018.10.119

Liu, M., Liu, M., Chen, W., and Yan, J. (2023). Operational flexibility and operation optimization of CHP units supplying electricity and two-pressure steam. Energy 263, 125988. doi:10.1016/j.energy.2022.125988

Liu, X., Qi, H., Ren, M., and Cheng, L. (2020). "A prediction method of NOx in thermal power plants using GC-LSTM neural network," in Proceedings of the 2020 Chinese Automation Congress, CAC 2020, Institute of Electrical and Electronics Engineers Inc., Shanghai, China, November, 2020, 3508–3512. doi:10.1109/CAC51589.2020.9327374

Liu, Z., Li, J., Zhang, P., Ding, Z., and Zhao, Y. (2022). An AGC dynamic optimization method based on proximal policy optimization. Front. Energy Res 10, 947532. doi:10.3389/fenrg.2022.947532

Peng, B., Ma, X., Ma, X., Tian, C., and Sun, Y. (2023). Coordinated AGC control strategy for an interconnected multi-source power system based on distributed model predictive control algorithm. Front. Energy Res 10, 1019464. doi:10.3389/fenrg.2022.1019464

Peng, D., Xu, Y., and Zhao, H. (2019). Research on intelligent predictive AGC of a thermal power unit based on control performance standards. Energies 12 (21), 4073. doi:10.3390/en12214073

Ramírez-Gallego, S., Lastra, I., Martínez-Rego, D., Bolón-Canedo, V., Benítez, J. M., Herrera, F., et al. (2016). Fast-mRMR: fast minimum redundancy maximum relevance algorithm for high-dimensional big data. Int. J. Intelligent Syst. Cell. 32 (2), 134–152. doi:10.1002/int.21833

Sahin, S. O., and Kozat, S. S. (2019). Nonuniformly sampled data processing using LSTM networks. IEEE Trans. Neural Netw. Learn. Syst. 30 (5), 1452–1461. doi:10.1109/TNNLS.2018.2869822

Stevanovic, V. D., Ilic, M., Djurovic, Z., Wala, T., Muszynski, S., and Gajic, I. (2018). Primary control reserve of electric power by feedwater flow rate change through an additional economizer – a case study of the thermal power plant "Nikola Tesla B". Energy 147, 782–798. doi:10.1016/j.energy.2018.01.102

Wang, D., Han, X., Li, H., and Li, X. (2023b). Modeling and control method of combined heat and power plant with integrated hot water storage tank. Appl. Therm. Eng. 226, 120314. doi:10.1016/j.applthermaleng.2023.120314

Wang, D., Xie, X., Zhou, Y., Han, X., and Si, L. (2023a). Improved coordinated control strategy of coal-fired power units with coupled heat storage based on supercritical carbon dioxide cycle. Appl. Therm. Eng. 230, 120850. doi:10.1016/j.applthermaleng.2023.120850

Wang, J., Pang, X., Gao, S., Zhao, Y., and Cui, S. (2019a). Assessment of automatic generation control performance of power generation units based on amplitude changes. *Int. J. Electr. Power & Energy Syst.* 108, 19–30. doi:10.1016/j.ijepes.2018.12.046

Wang, R., Liu, H., Niu, Y., and Gu, Z. (2017). Study on PID parameters optimization based on performance indexes of AGC. *J. Eng. Therm. Energy Power* 32 (7), 58–63. doi:10.16146/j.cnki.rndlgc.2017.07.009

Wang, X., Tao, Y., and Zheng, K. (2018). "Feature selection methods in the framework of mRMR," in Proceedings of the 8th International Conference on Instrumentation and Measurement, Computer, Communication and Control (IMCCC), Institute of Electrical and Electronics Engineers Inc., Harbin, Heilongjiang, China, July, 2018, 1490–1495. doi:10.1109/IMCCC.2018.00307

Wang, Y., Cao, L., Hu, P., Li, B., and Li, Y. (2019b), Model establishment and performance evaluation of a modified regenerative system for a 660 MW supercritical unit running at the IPT-setting mode, *Energy*, 179,890–915. doi:10.1016/j.energy.2019.05.026

Wang, Z., Jia, L., and Ren, C. (2021). "Attention-bidirectional LSTM based short term power load forecasting," in Proceedings of the Institute of Electrical and Electronics Engineers Inc., Virtual, Online, China, August, 2021, 171–175. doi:10.1109/PSGEC51302.2021.9541781

Xi, L., Zhou, L., Lang, L., Duan, D., Xu, Y., Yang, L., et al. (2020). A deep reinforcement learning algorithm for the power order optimization allocation of AGC in interconnected power grids. *CSEE J. Power Energy Syst. (JPES)* 6 (3), 712–723. doi:10.17775/CSEEJPES.2019.01840

Yang, C., Sun, W., Han, D., and Yin, X. (2022). Research on power system flexibility considering uncertainties. *Front. Energy Res.* 10, 967220. doi:10.3389/fenrg.2022.967220

Yin, J., Liu, M., and Yan, J. (2022). Effect of fuel side deviations on the load-cycling performance of thermal power plants: a dynamic simulation. *Appl. Therm. Eng.* 206, 118041. doi:10.1016/j.applthermaleng.2022.118041

Yu, Y., Si, X., Hu, C., and Zhang, J. (2019). A review of recurrent neural networks: LSTM cells and network architectures. *Neural Comput.* 31 (7), 1235–1270. doi:10.1162/neco_a_01199

Yuan, X., Chen, C., Jiang, M., and Yuan, Y. (2019). Prediction interval of wind power using parameter optimized Beta distribution based LSTM model. *Appl. Soft Comput. J.* 82, 105550. doi:10.1016/j.asoc.2019.105550

Zhang, K., Zhao, Y., Liu, M., Gao, L., Fu, Y., and Yan, J. (2021). Flexibility enhancement versus thermal efficiency of coal-fired power units during the condensate throttling processes. *Energy* 218 (1), 119534. doi:10.1016/j.energy.2020.119534

Zhang, Y., Wang, S., and Ji, G. (2015). A comprehensive survey on particle swarm optimization algorithm and its applications. *Math. Problems Eng.* 2015, 1–38. doi:10.1155/2015/931256

Zhou, T., Chen, L. F., Bu, S. Q., Ye, H., and Sun, J. (2023). Dominant mode identification and influence mechanism investigation of frequency oscillations as affected by automatic generation control. *Int. J. Electr. Power & Energy Syst.* 148, 108981. doi:10.1016/j.ijepes.2023.108981